

Atom Laser with a cw Output Coupler

Immanuel Bloch, Theodor W. Hänsch, and Tilman Esslinger

*Sektion Physik, Ludwig-Maximilians-Universität, Schellingstrasse 4/III, D-80799 Munich, Germany
and Max-Planck-Institut für Quantenoptik, D-85748 Garching, Germany*

(Received 3 December 1998)

We demonstrate a continuous output coupler for magnetically trapped atoms. Over a period of up to 100 ms, a collimated and monoenergetic beam of atoms is continuously extracted from a Bose-Einstein condensate. The intensity and kinetic energy of the output beam of this atom laser are controlled by a weak rf field that induces spin flips between trapped and untrapped states. Furthermore, the output coupler is used to perform a spectroscopic measurement of the condensate, which reveals the spatial distribution of the magnetically trapped condensate and allows manipulation of the condensate on a micrometer scale. [S0031-9007(99)08914-0]

PACS numbers: 03.75.Fi, 05.30.Jp, 32.80.Pj, 42.55.-f

Four decades ago the first optical lasers [1] were demonstrated [2,3], marking a scientific breakthrough: Ultimate control over frequency, intensity, and direction of optical waves had been achieved. Since then, lasers have found innumerable applications, for both scientific and general use. It may now be possible to control matter waves in a similar way, as Bose-Einstein condensation (BEC) has been attained in a dilute gas of trapped atoms [4–6]. In a Bose-Einstein condensate a macroscopic number of bosonic atoms occupy the ground state of the system, which can be described by a single wave function. A pulsed output coupler which coherently extracts atoms from a condensate was demonstrated recently [7,8]. Because of its properties, this source is often referred to as an atom laser.

In this Letter we report on the successful demonstration of an atom laser with a continuous output. The duration of the output is limited only by the number of atoms in the condensate. The Bose-Einstein condensate is produced in a novel magnetic trap [9] which provides an extremely stable trapping potential. A weak rf field is used to extract the atoms from the condensate over a period of up to 100 ms, thereby forming an atomic beam of unprecedented brightness. The output coupling mechanism can be visualized as a small, spatially localized leak in the trapping potential. The condensate wave function passes through the leak and forms a collimated atomic beam. This continuous output coupler allows the condensate wave function to be studied and manipulated with high spatial resolution.

Let us consider a simple model for a cw output coupler [10–12] and assume that atoms which are in a magnetically trapped state are transferred into an untrapped state by a monochromatic resonant rf field. In the untrapped state the atoms experience the repulsive mean-field potential of the condensate, which can be approximated by the parabolic form of a Thomas-Fermi distribution. When the atoms leave the trap the corresponding potential energy of the atoms is transformed into kinetic energy. The velocity of the atoms leaving the trap can be adjusted by the frequency

of the rf field, because it determines the spatial region where the atoms are transferred into the untrapped state.

So far, only pulsed output couplers have been demonstrated [7,13,14]. If a short and, hence, broadband rf pulse is applied, the output pulse has a correspondingly large energy spread. Each portion of the condensate that leaves the trap has a kinetic energy distribution with a width comparable to the mean-field energy of the condensate. For this case the output coupling process is no longer spatially selective and therefore largely insensitive to fluctuations in the magnetic field.

Continuous wave output coupling, as done in this paper, can be achieved only if the magnetic field fluctuations that the trapped atoms experience are minimized. The level of fluctuations in the magnetic field has to be much less than the change of the magnetic trapping field over the spatial size of the condensate.

In the experiment, we use a novel magnetic trap [9], the quadrupole and the Ioffe configuration (QUIC) trap, which is particularly compact and operates at a current of just 25 A. The compactness of the trap allowed us to place it inside a μ -metal box, which reduces the magnetic field of the environment and its fluctuations by a factor of approximately 100. In combination with an extremely stable current supply ($\Delta I/I < 10^{-4}$) we are able to reduce the residual fluctuations in the magnetic field to a level below 0.1 mG. The rf field for the output coupler is produced by a synthesizer (HP-33120A) and is radiated from the same coil as is used for evaporative cooling. The coil has 10 windings, a diameter of 25 mm, and is mounted 30 mm away from the trap center. The magnetic field vector of the rf is oriented in the horizontal plane, perpendicular to the magnetic bias field of the trap.

To obtain Bose-Einstein condensates we use the same setup and experimental procedure as in our previous paper [9]. Typically, 10^9 rubidium atoms are trapped and cooled in a magneto-optical trap. Then the atoms are transferred into the QUIC trap where they are further cooled by rf-induced evaporation. The QUIC trap is operated with

trapping frequencies of $\omega_{\perp} = 2\pi \times 180$ Hz in the radial and $\omega_y = 2\pi \times 19$ Hz in the axial direction. In this configuration the trap has a magnetic field of 2.5 G at its minimum.

After the creation of the Bose-Einstein condensate, the rf field used for evaporative cooling is switched off, and 50 ms later the radio frequency of the output coupler is switched on for a time of 15 ms in a typical experiment. The field of the output coupler is ramped up to an amplitude of $B_{\text{rf}} = 2.6$ mG within 0.1 ms. Its frequency follows a linear ramp from 1.752 to 1.750 MHz, to account for the shrinking size of the condensate, as discussed below. Over this period, atoms are extracted from the condensate and are accelerated by gravity. Subsequently, the magnetic trapping field is switched off, and 3.5 ms later the atomic distribution is measured by absorption imaging. The atom laser output is shown in Fig. 1. The beam contains 2×10^5 atoms and its divergence in the plane of observation is below our experimental resolution limit of 3.5 mrad. We obtain an output beam over a longer period of time when we reduce the magnetic field amplitude B_{rf} of the rf field. With absorption imaging we are able to directly image the

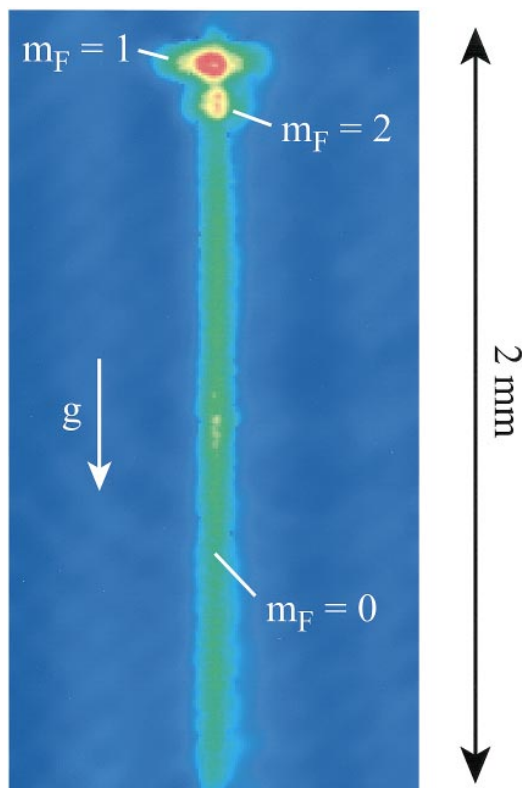


FIG. 1(color). Atom laser output: A collimated atomic beam is derived from a Bose-Einstein condensate over a 15 ms period of continuous output coupling. A fraction of condensed atoms has remained in the magnetically trapped $|F = 2, m_F = 2\rangle$ and $|F = 2, m_F = 1\rangle$ state. The magnetic trap has its weakly confining axis in the horizontal direction.

continuous output from the atom laser over 40 ms, with $B_{\text{rf}} = 1.2$ mG. A more sensitive method is to measure the number of atoms that remain in the condensate after a certain period of time. This enables us to monitor the output coupling process over up to 100 ms, with $B_{\text{rf}} = 0.2$ mG. The magnetic field amplitudes have been calibrated with an accuracy of 20%.

It is instructive to estimate the brightness of the beam produced by our atom laser. Defining the brightness as the integrated flux of atoms per source size divided by the velocity spreads in each dimension $\Delta v_x \Delta v_y \Delta v_z$ [15], we find that the brightness of our beam has to be at least 2×10^{24} atoms $\text{s}^2 \text{m}^{-5}$. To obtain this lower limit for the brightness, we estimate that the atomic flux is 5×10^6 atoms/s and that the longitudinal velocity spread is given by $\Delta v_z = 3$ mm/s. We further assume a velocity spread $\Delta v_x = 5$ mm/s for the strongly confining axis, which corresponds to the chemical potential of the condensate. Our measurements show that the velocity spread along the weakly confining axis is less than $\Delta v_y = 0.3$ mm/s.

Assuming a Fourier-limited longitudinal velocity width of $\Delta v_z = 0.3$ mm/s and diffraction-limited transverse velocity spreads, a brightness of 4×10^{28} atoms $\text{s}^2 \text{m}^{-5}$ can be reached. Both numbers show that continuous output coupling from a condensate creates an atomic beam with a brightness that is orders of magnitude higher than that of a state-of-the-art Zeeman, slower [18] with a brightness of 2.9×10^{18} atoms $\text{s}^2 \text{m}^{-5}$, or an atomic source derived from a magneto-optical trap [19], with a brightness of 8.5×10^{16} atoms $\text{s}^2 \text{m}^{-5}$.

Let us now consider the geometry of the trap with respect to the output coupling mechanism in more detail. The magnetic field $B(\mathbf{r})$ gives rise to a harmonic trapping potential which confines the condensate in the shape of a cigar, with its long axis oriented perpendicular to the gravitational force. The rf field of frequency ν_{rf} induces transitions from the magnetically trapped $|F = 2, m_F = 2\rangle$ state to the untrapped $|F = 2, m_F = 0\rangle$ state via the $|F = 2, m_F = 1\rangle$ state. Here F denotes the total angular momentum and m_F is the magnetic quantum number. The resonance condition $\frac{1}{2} \mu_B |B(\mathbf{r})| = h \nu_{\text{rf}}$, where μ_B is the Bohr magneton, is satisfied on the surface of an ellipsoid which is centered at the minimum in the magnetic trapping field [20]. Without gravity the condensate would have the same center, so that an undirected output could be expected [11]. The frequency range in which significant output coupling occurs would then be determined by the magnetic field minimum B_{off} and by the chemical potential μ of the condensate: $\frac{1}{2} \mu_B B_{\text{off}} \leq h \nu_{\text{rf}} \leq \frac{1}{2} (\mu_B B_{\text{off}} + \mu)$.

Because of gravity, the minimum of the trapping potential is displaced relative to the minimum of the magnetic field. With g being the gravitational acceleration, this displacement is given by g/ω_{\perp}^2 , which is $7.67 \mu\text{m}$ for our trapping parameters. The confinement of the trap

and hence the spatial size of the condensate remain the same. In this geometry, which is illustrated in Fig. 2, output coupling occurs only at the intersection of the displaced condensate with the ellipsoid that is determined by the resonance condition. Atoms leaving the condensate therefore experience a directed force which is dominated by gravity in our experiment and gives rise to a collimated output beam. The frequency range over which output coupling can be achieved is larger than without gravity, because the condensate is shifted into a region of an increasingly stronger magnetic field gradient. The frequency interval $\Delta\nu = g\sqrt{2\mu m}/(h\omega_{\perp})$, where m is the atomic mass, gives the difference in frequency between an rf field that is resonant with the upper edge and an rf field that is resonant with the lower edge of the condensate, assuming a Thomas-Fermi distribution. For our trapping parameters and 7×10^5 rubidium atoms in the condensate this frequency interval is $\Delta\nu = 10.2$ kHz.

We investigate the condensate spectroscopically by measuring the number of atoms which remains in the condensate after 20 ms of output coupling, for various amplitudes and frequencies of the rf field. The number of atoms in the condensate is measured by absorption imaging. Before the absorption pulse is applied, the condensate is released from the magnetic trap and expands ballistically for 10.5 ms. Because of an inhomogeneous magnetic field, which is applied during the switch-off period, atoms in the $m_F = 2$ and $m_F = 1$ magnetic sublevel are spatially separated from each other, allowing us to determine the population in each of the sublevels independently (see also Fig. 1). The experimental parameters are carefully controlled for each series of measurements, so that the number of atoms in the condensate does not fluctuate by more than 5%.

In Fig. 3 the number of atoms in the condensate is plotted versus the square of the Rabi frequency which

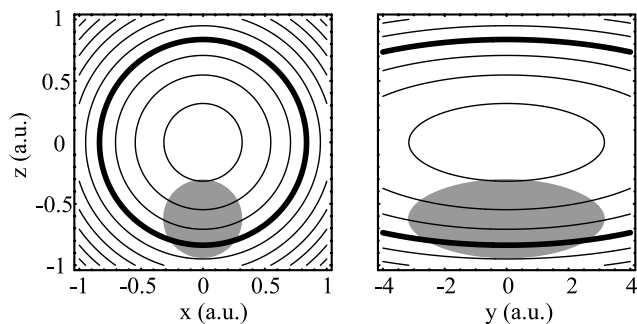


FIG. 2. Continuous output coupling from a Bose-Einstein condensate. The contour lines represent the absolute value of the magnetic trapping field. The thick line indicates the region where the rf field transfers atoms from the magnetically trapped state into an untrapped state. Because of gravity, the condensate is trapped $7.67 \mu\text{m}$ below the minimum in the magnetic field. In the untrapped state the atoms experience a directed force caused by gravity and the mean field of the condensate. This results in a collimated output beam.

is induced by the rf field, for a fixed frequency of 1.736 MHz. With increasing rf power the population N in the condensate decreases until it approaches a constant level N_0 . This is to be expected, since the size of the condensate shrinks with its depopulation until the overlap with the resonance ellipsoid vanishes. Our measurements can therefore be explained by the simple rate equation $\frac{dN(t)}{dt} = -\Gamma[N(t) - N_0]$, in which the depopulation rate Γ is proportional to the square of the Rabi frequency $\Omega = g_F \mu_B B / \hbar$, with g_F being the Landé factor. From a fit to our experimental data we obtain $\Gamma/\Omega^2 = 1.2(2) \times 10^{-5}$ s.

Figure 4 shows the dependency of the condensate population on the frequency of the rf field, for $\Omega = 2\pi \times 0.7$ kHz. The measured distribution has a width of 13.1(5) kHz (10% values) and stretches over a larger frequency range than the 10.2 kHz estimated (see above). This is to be expected, since the Thomas-Fermi distribution does not properly take into account the decay of the wave function near the outer edge of the condensate. The condensate wave function extends beyond the classical radius R , determined by the Thomas-Fermi distribution, and falls off exponentially on a characteristic length scale, which is given by $\delta = R/2(\hbar\omega_{\perp}/\mu)^{2/3}$ [21,22]. For our parameters we obtain $\delta/R = 0.074$. Our measurements are in good agreement with these considerations. The slight asymmetry of the measured curve is caused by the asymmetry in the number of atoms per resonance ellipsoid.

The results clearly show the high spectral and spatial resolution of our output coupler. From an estimated spectral resolution of 1 kHz we obtain a spatial resolution of about $1 \mu\text{m}$. A more precise comparison of our measurements with a theoretical model [11,12] should be possible if the magnetic structure of the $F = 2$ spin state is taken into account and if the output coupling process is studied beyond the Thomas-Fermi approximation.

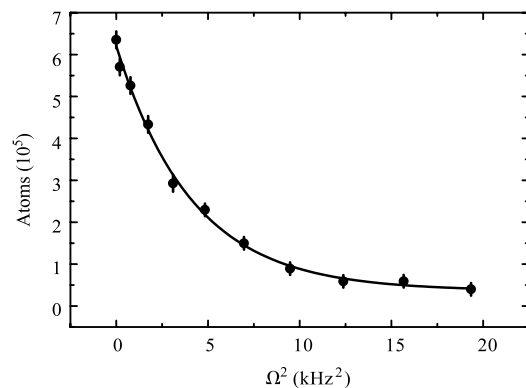


FIG. 3. Condensate population of the $|F = 2, m_F = 2\rangle$ state after a 20 ms period of output coupling versus the square of the Rabi frequency induced by the rf field. The solid line represents a fit based on a simple rate equation model (see text).

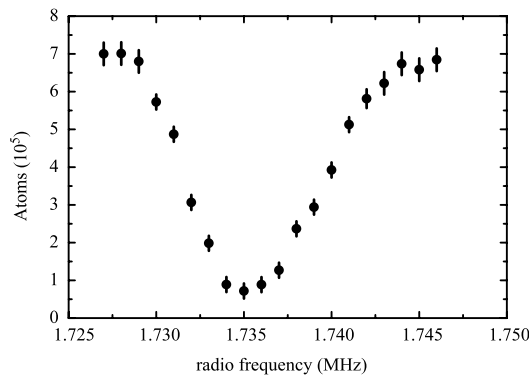


FIG. 4. Spectroscopy of the Bose-Einstein condensate. The condensate population of the $|F = 2, m_F = 2\rangle$ state is shown for different radio frequencies after a 20 ms period of output coupling. Assuming a Thomas-Fermi distribution for the condensate density we expect output coupling to occur within a frequency interval of 10.2 kHz (see text). This does not take into account the exponential decay of the condensate wave function at the surface of the condensate.

The method reported in this paper is a starting point to systematically analyze the spectroscopic properties of alkali condensates [23]. Our experiments also demonstrate that Bose-Einstein condensates can be manipulated on a micrometer scale with rf fields. A similar scheme to our output coupler could be used to realize a weak link between two condensates which are trapped in different internal states [24]. This would provide the means to observe Josephson-type oscillations, as discussed in a recent theoretical paper [25].

Studies on the output properties of the atom laser will provide a fascinating field of research. It has already been shown that the rf output coupling process preserves first order coherence [8], but more quantitative and detailed measurements are required. One of the crucial properties of an optical laser is its second order coherence [26]. A direct measurement of the second order coherence of an atom laser would reveal the intriguing consequences of quantum statistics.

There is a wide range of applications for atom lasers in the field of atom optics. It is now conceivable to produce diffraction-limited atomic beams which could be focused down to a spot size of much less than 1 nm. Atom lasers will also revolutionize atom interferometers. Highly collimated and slow beams of atoms, as demonstrated in this paper, make it possible to create atom interferometers with large enclosed areas and a superior signal-to-noise ratio, which are ideally suited for precision measurements.

We would like to thank Jens Schneider for stimulating discussions.

- [1] A. L. Schawlow and C. H. Townes, *Phys. Rev.* **112**, 1940 (1958).
- [2] T. H. Maiman, *Nature (London)* **187**, 493 (1960).
- [3] A. Javan, W. B. Bennett, Jr., and D. R. Herriott, *Phys. Rev. Lett.* **6**, 106 (1961).
- [4] M. H. Anderson *et al.*, *Science* **269**, 198 (1995).
- [5] C. C. Bradley, C. A. Sackett, J. J. Tollett, and R. G. Hulet, *Phys. Rev. Lett.* **75**, 1687 (1995); C. C. Bradley, C. A. Sackett, and R. G. Hulet, *Phys. Rev. Lett.* **78**, 985 (1997).
- [6] K. B. Davis *et al.*, *Phys. Rev. Lett.* **75**, 3969 (1995).
- [7] M.-O. Mewes *et al.*, *Phys. Rev. Lett.* **78**, 582 (1997).
- [8] M. R. Andrews *et al.*, *Science* **275**, 637 (1997).
- [9] T. Esslinger, I. Bloch, and T. W. Hänsch, *Phys. Rev. A* **58**, R2664 (1998).
- [10] R. J. Ballagh, K. Burnett, and T. F. Scott, *Phys. Rev. Lett.* **78**, 1607 (1997).
- [11] M. Naraschewski, A. Schenzle, and H. Wallis, *Phys. Rev. A* **56**, 603 (1997).
- [12] H. Steck, M. Naraschewski, and H. Wallis, *Phys. Rev. Lett.* **80**, 1 (1998).
- [13] B. P. Anderson and M. A. Kasevich, *Science* **282**, 1686 (1998).
- [14] K. Helmerson *et al.* (private communication).
- [15] In this, we follow the definition of [16] and additionally include the source size of the beam, as is usual for the definition of the brightness of a light source in optics [17].
- [16] E. Riis, D. S. Weiss, K. A. Moler, and S. Chu, *Phys. Rev. Lett.* **64**, 1658 (1990).
- [17] L. Mandel and E. Wolf, *Optical Coherence and Quantum Optics* (Cambridge University Press, Cambridge, England, 1995).
- [18] D. Meschede (private communication).
- [19] Z. T. Lu *et al.*, *Phys. Rev. Lett.* **77**, 3331 (1996).
- [20] Using the Breit-Rabi formula, we equate that the magnetic splitting between the $m_F = 0$ and $m_F = 1$ state is 900 Hz larger than the splitting between the $m_F = 1$ and $m_F = 2$ state.
- [21] F. Dalfovo, L. Pitaevskii, and S. Stringari, *Phys. Rev. A* **54**, 4213 (1996).
- [22] E. Lundh, C. J. Pethick, and H. Smith, *Phys. Rev. A* **55**, 2126 (1997).
- [23] Two-photon optical spectroscopy was recently used to observe BEC in atomic hydrogen. See T. C. Killian *et al.*, *Phys. Rev. Lett.* **81**, 3807 (1998); D. G. Fried *et al.*, *Phys. Rev. Lett.* **81**, 3811 (1998).
- [24] D. S. Hall *et al.*, *Phys. Rev. Lett.* **81**, 1539 (1998); D. S. Hall, M. R. Matthews, C. E. Wieman, and E. A. Cornell, *Phys. Rev. Lett.* **81**, 1543 (1998); M. R. Matthews *et al.*, *Phys. Rev. Lett.* **81**, 243 (1998).
- [25] J. Williams, R. Walser, J. Cooper, E. Cornell, and M. Holland, *Phys. Rev. A* **59**, R31 (1999).
- [26] F. T. Arecchi, E. Gatti, and A. Sona, *Phys. Lett.* **20**, 27 (1966).